Dynamics of functionalized single wall carbon nanotubes in solution studied by incoherent neutron scattering experiments

2008 J. Phys.: Condens. Matter 20 104208

(http://iopscience.iop.org/0953-8984/20/10/104208)

J. Phys.: Condens. Matter **20** (2008) 104208 (6pp) doi:10.1088/0953-8984/20/10/104208

Dynamics of functionalized single wall carbon nanotubes in solution studied by incoherent neutron scattering experiments

A Urbina[1], C Miguel[1], J L Delgado[2], F Langa[2], C Díaz-Paniagua[3], M Jiménez[4] and F Batallán[5]

[1] Departamento Electrónica, Universidad Politécnica de Cartagena, Plaza Hospital 1, 30202 Cartagena, Spain
[2] Facultad de Ciencias del Medio Ambiente, Universidad de Castilla-La Mancha, 45071, Toledo, Spain
[3] Centro Español de Metrología, 28760 Madrid, Spain
[4] Institut Laue-Langevin, 39042 Grenoble Cedex, France
[5] Instituto de Ciencia de Materiales de Madrid, CSIC, 28049 Madrid, Spain

E-mail: antonio.urbina@upct.es

Received 13 July 2007, in final form 28 September 2007
Published 19 February 2008
Online at stacks.iop.org/JPhysCM/20/104208

Abstract

We have studied, by incoherent neutron scattering experiments, the dynamics of a colloidal suspension of functionalized single wall carbon nanotubes (SWNTs). The nanotubes have been functionalized with pentyl ester groups attached at the ends and suspended in deuterated toluene with a concentration of 2.6 mg SWNT/1 ml of deuterated toluene. The experimental techniques were incoherent elastic neutron scattering (IENS) and incoherent quasielastic neutron scattering (IQNS). In the temperature range between 4 K and 300 K, three phases were observed by IENS measurements: a solid phase for $T < T_g$, an undercooled liquid phase for $T_g < T < T_m$ and a liquid phase for $T > T_m$. Furthermore, in the high temperature range of the undercooled liquid phase, hysteresis loops in the heating and cooling scans were observed. The lower limit of the hysteresis loop defines the critical crossover temperature T_c. IQNS measurements in the liquid phase and a cooling scan of the undercooled liquid phase were performed. Three different quasielastic peaks were identified, two in the liquid phase and another one in the undercooled liquid phase. The widths of the quasielastic peaks are discussed as a generalized diffusion function which can be factorized as a temperature dependent diffusion function and a Q dependent structure function. From the comparison of the diffusion function with the viscosity of toluene, we conclude that two components are in the long-time range Brownian motion and the other one in the short-time range Brownian motion.

1. Introduction

Functionalized single wall carbon nanotubes (f-SWNTs) dispersed in deuterated toluene are a colloidal suspension. The size of the f-SWNT colloidal particles is generally larger than the size of the solvent molecules but still small enough so that their mobility is governed by thermally activated Brownian motion. Colloidal particles are, however, also subject to attractive Van der Waals forces, leading to irreversible aggregation. In order to balance this effect, the particles need to be stabilized and several schemes have been developed to do so, such as charge or steric stabilization. Steric stabilization of a colloidal dispersion is achieved by attaching polymer chains to colloidal particles. Then when colloidal particles approach one another the limited interpenetration of the polymer chain leads to an effective repulsion which stabilizes the dispersion against flocculation or coagulation. One approach for stabilizing a colloidal system is the functionalization of the particles with short polymeric chains (as compared to the particle size) grafted to the end of the particles.

Our recent developments have allowed us to prepare stable solutions of functionalized carbon nanotubes in different solvents. These samples are SWNTs with –COOH radicals at

the ends, the hydrogen can be substituted by short saturated chains of carbons, which improves their solubility in organic solvents and also enhances the neutron scattering signal of the carbon nanotube [1, 2]. This approach is different from previous neutron scattering measurements of carbon nanotubes, such as inelastic neutron scattering (INS) at low energies (0–225 meV) that has been performed on solid samples [3–5] or small angle neutron scattering (SANS) measurements that were performed on SWNTs in a dilute suspension in water using surfactants [6, 7]. Measurements of functionalized SWNTs suspended without the help of surfactants are important since fabrication of devices by spin-coating or drop-casting of materials from a liquid solution or suspension is now a common procedure for optoelectronic organic applications using blends of nanotubes and polymers [8–10].

The structure of a colloidal suspension can be described in terms of the static structure factor $S(Q)$. In a dilute suspension, there are no interparticle correlations and $S(Q) = 1$. There are nevertheless dynamics in the sample and the colloidal particles move by the thermal fluctuation of the solvent. For concentrated systems, where interparticle correlations play a role, the static structure factor $S(Q)$ deviates from unity and shows pronounced features, including a peak $S(Q_{\max})$ that is related to the mean interparticle spacing by $2\pi/Q_{\max}$. The exact functional form of $S(Q)$ will depend on the nature of the interactions occurring in the system.

The dynamic behaviour in a dilute suspension is given by the Stokes–Einstein diffusion coefficient D_{SE}. For a functionalized carbon nanotube of radius R and cylindrical axis L, the Stokes–Einstein relation is given by the expression:

$$D_{\mathrm{SE}}(T) = \frac{2k_{\mathrm{B}}T}{9\pi L\eta_0(T)}, \tag{1}$$

where k_{B} is the Boltzmann constant, T the temperature and η_0 the shear viscosity of the suspending fluid, and $L \gg R$ for the nanotubes. For concentrated systems, the dynamic behaviour is more complex and involves not only the interactions of the colloidal particles with the solvent molecules but is also strongly dependent on the direct interactions between particles. On top of that, hydrodynamic interactions mediated by the suspending solvent have to be considered.

The motion of Brownian particles suspended in a liquid is characterized by three distinct time regimes [11]. For long times $\tau \gg \tau_{\mathrm{R}}$ their motion is diffusive, resulting from interactions with the surrounding fluid and random collisions with other particles. This is the Brownian long-time regime. The time $\tau_{\mathrm{R}} = R^2/D_{\mathrm{SE}}$ needed for a particle to diffuse over a distance comparable to its radius is an estimate of the timescale on which direct interaction between the particles becomes important

$$\tau_{\mathrm{R}} = \frac{9\pi L R^2\eta_0(T)}{2k_{\mathrm{B}}T}. \tag{2}$$

At shorter times $\tau_{\mathrm{B}} \ll \tau \ll \tau_{\mathrm{R}}$, the motion is also diffusive, but at a faster rate, reflecting the fact that the particles have not yet been slowed down by direct interaction with neighbouring particles. This is the Brownian short-time regime and the only interparticle interactions are the hydrodynamic interactions transmitted by the fluid. The Brownian relaxation time τ_{B} characterizes the time taken to decouple the dynamics of the colloidal particle from the dynamics of the fluid and is given by

$$\tau_{\mathrm{B}} = \frac{2m}{9\pi L\eta_0(T)}, \tag{3}$$

where m is the mass of the colloidal particle. At even shorter timescales $\tau \leqslant \tau_{\mathrm{B}}$ the motion of the particles evolves from ballistic to diffusive as the velocity imparted to the particles by the collision with the fluid molecules is viscously damped. This is the pre-Brownian time regime. There is a clear separation between the two times τ_{R} and τ_{B}, allowing for the definition of distinct short-and long-time dynamics. For long-time Brownian motion, the temperature dependence of the time is $\tau \propto \eta_0(T)/T$ and for the short-time Brownian motion $\tau \propto 1/\eta_0(T)$.

A descriptive picture of the dynamical process is often given in terms of cage diffusion. At short times, relatively rapid particle motions take place inside the cage of spheres that surround each particle. As time evolves, the spheres move far enough to encounter their neighbours, which serve to slow down their motions. At the longest times particles move through the constantly changing matrix of neighbour cages and the motions again are Brownian, although much reduced in rate as compared to the earliest times.

2. Experimental details

In this experiment we have performed neutron scattering measurements on stable solutions of functionalized SWNTs in deuterated toluene. We have functionalized the SWNTs with pentyl ester groups at the ends. This functionalization allowed us both to get stable solutions and to enhance the neutron scattering signal by protonation of the sample dissolved in a deuterated solvent (toluene). The samples were prepared starting from acid purified HIPco SWNTs containing carboxylic groups at their ends that were reacted first with thionyl chloride, followed by addition of n-pentanol. It resulted in n-pentyl ester groups attached at the ends of the nanotubes which make them soluble in toluene. Solutions of the nanotubes in deuterated toluene at different weight concentrations were prepared. Sample preparation details are given in [1] and [2]. In this experiment we have studied two samples: fully deuterated toluene, D8 (sample T) and functionalized SWNTs with pentyl ester groups at the ends and concentration 2.6 mg SWCN/1 ml of deuterated toluene (sample C).

Neutron scattering measurements were performed at the Institut Laue-Langevin in Grenoble, France. Provided that the Bragg peaks are avoided, the scattering intensity is almost entirely incoherent and it was dominated by the incoherent scattering cross section of H. Two different spectrometers were used: the IN10 backscattering spectrometer and the IN6 time of flight spectrometer. The experimental Q range covered by both instruments is from 0.4 to 2 $\mathrm{\AA}^{-1}$.

Incoherent elastic neutron scattering (IENS) measurements using the fixed elastic window configuration of the IN10

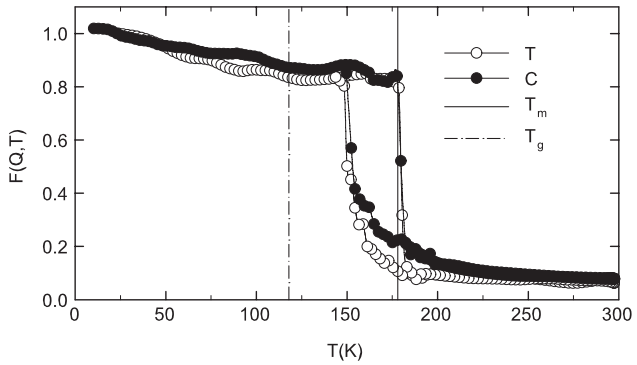

Figure 1. The IENS measurement in a heating and cooling scan in the 10 to 300 K temperature range at $Q = 0.86$ Å^{-1} for the C and T samples. An hysteresis loop is observed in the undercooled liquid phase.

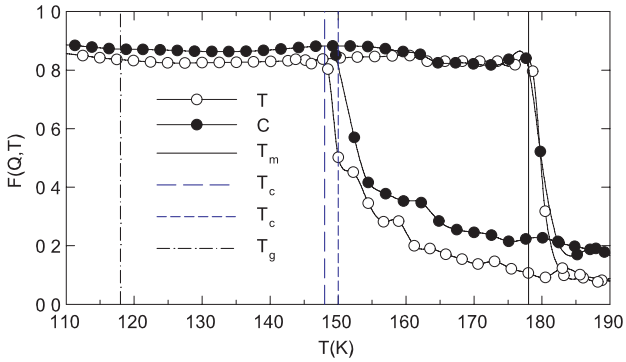

Figure 2. Detail of the hysteresis loop in the undercooled liquid phase observed by IENS measurement in a heating and cooling scan for the C and T samples. If T_m is the same for both samples, T_c given by the low temperature limit of the hysteresis loop is different for each sample.

neutron backscattering spectrometer for heating and cooling scans were realized. A slow temperature variation assured quasi-equilibrium conditions. If $I(Q, T)$ is the elastic intensity, the elastic incoherent structure factor (EISF) is given by $F(Q, T) = I(Q, T)/I(Q, T_0)$ with T_0 a low temperature where it is assumed there is no quasielastic broadening.

Incoherent quasielastic neutron scattering (IQNS) measurements have been performed at selected temperatures with the backscattering spectrometer IN10 and the time of flight spectrometer IN6. The experimental energy range of the IN10 backscattering spectrometer was from -12 to 12 μeV with a resolution of about 1 μeV and that of the IN6 time of flight spectrometer was from -4 to 60 meV with a resolution of about 50 μeV.

3. Results and discussion

The IENS measurements were performed with the IN10 backscattering spectrometer in the fixed elastic window configuration. We made heating and cooling scans between 10 and 300 K at a low temperature rate of 0.62 K min^{-1} and $I(Q, T)$ was recorded for each Q.

The thermal variation of $F(Q, T)$ over the range 10–300 K for both samples is shown in figure 1. We have superimposed the two critical temperatures of toluene: the glass transition temperature $T_g = 118$ K and the melting temperature $T_m = 178$ K [12]. These allow us to define three temperature ranges: $T < T_g$ solid phase, $T > T_m$ liquid phase and $T_g < T < T_m$ undercooled liquid phase. The main characteristic of the thermal variation of $F(Q, T)$ is the presence of a hysteresis loop in the undercooled liquid phase. The mode coupling theory of the glass transition predicts a critical temperature T_c in the undercooled liquid phase associated with a tendency for change in the viscosity behaviour [13]. From neutron scattering measurements in toluene this temperature was estimated at $T_c = 144$ K [14]. This critical temperature allows us to define two regions in the undercooled liquid phase: $T_c < T < T_m$ and $T_g < T < T_c$.

Figure 2 shows the detail of $F(Q, T)$ in the temperature range between 110 and 190 K, covering the undercooled liquid phase. In the high temperature range of the undercooled liquid phase the hysteresis loop is observed. The two limits of the hysteresis loop allow us to define T_m by the upper limit and T_c by the lower limit, defining $T_c < T < T_m$ as the high temperature range of the undercooled liquid phase. If T_m is the same for both samples, this is not the case for T_c; we have $T_c = 148$ K for sample T and $T_c = 150$ K for sample C.

The variation of the IENS function $F(Q, T)$ (figure 1) allows us to define two regions in the experimental temperature range. For the heating scan in the temperature range $T < T_m$, $F(Q, T)$ varies between 1 and 0.8, however, for the cooling scan in the temperature range $T > T_c$, $F(Q, T)$ varies between 0 and 0.2.

The IQNS measurements were carried out on the time of flight spectrometer IN6 and the backscattering spectrometer IN10 covering the high temperature range. The liquid phase was measured on IN6 and the cooling scan of the high temperature range of the undercooled liquid phase on IN10. These quasielastic peaks were fitted with an incoherent scattering function $S_{inc}(Q, \omega)$ formed by a delta elastic function and two Lorentzian quasielastic functions of half-width at the half-maximum (HWHM), $\Gamma_1(Q, T)$ and $\Gamma_2(Q, T)$. We convoluted the model with the experimental resolution given by the experimental IQNS of vanadium and the result was compared with the corresponding experimental IQNS spectrum at a given temperature.

The second IQNS measurements were performed with the IN10 spectrometer in the cooling scan of the high temperature range of the undercooled liquid phase. The two samples were studied at three temperatures: 165, 160 and 155 K. These data were fitted by an incoherent scattering function $S_{inc}(Q, \omega)$ formed by Lorentzian quasielastic functions of HWHM $\Gamma_0(Q, T)$.

In figure 3 are shown the two HWHM of the Lorentzian quasielastic peaks $\Gamma_1(Q, T)$ and $\Gamma_2(Q, T)$ as a function of Q for several temperatures in the liquid phase and $\Gamma_0(Q, T)$ as a function of Q for several temperatures in the cooling branch of the undercooled liquid phase.

Three motions have been identified: (a) a classical diffusion motion in an extended volume with a characteristic width $\Gamma_0(Q, T)$ with a strong Q dependence, (b) a motion in

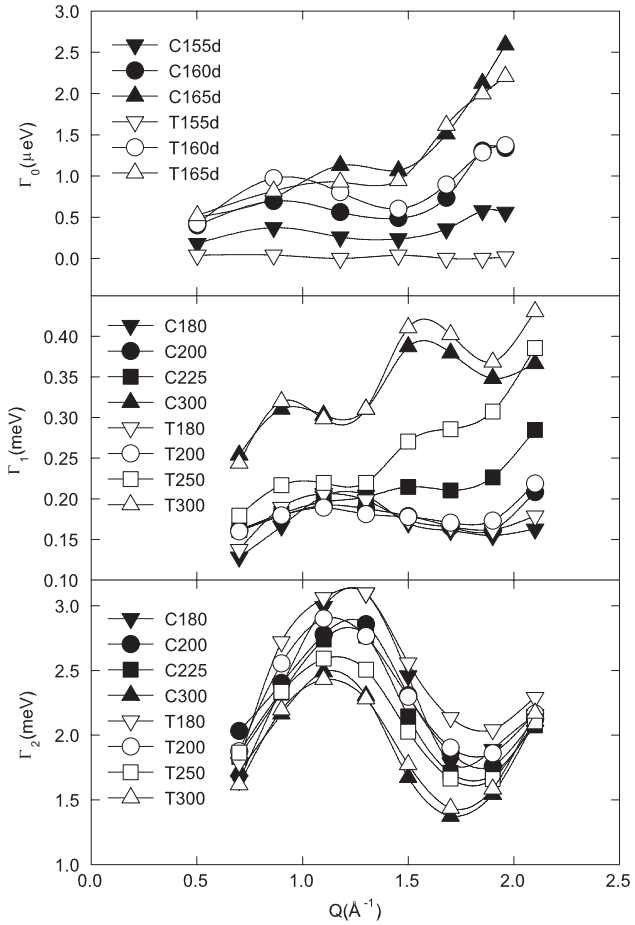

Figure 3. The HWHM of the Lorentzian quasielastic peak, Γ, as a function of Q at several temperatures. Γ_0 was measured in the cooling branch of the hysteresis loop in the undercooled liquid region and Γ_1 and Γ_2 in the liquid region (lines are drawn as a guide to the eye, but have no theoretical significance).

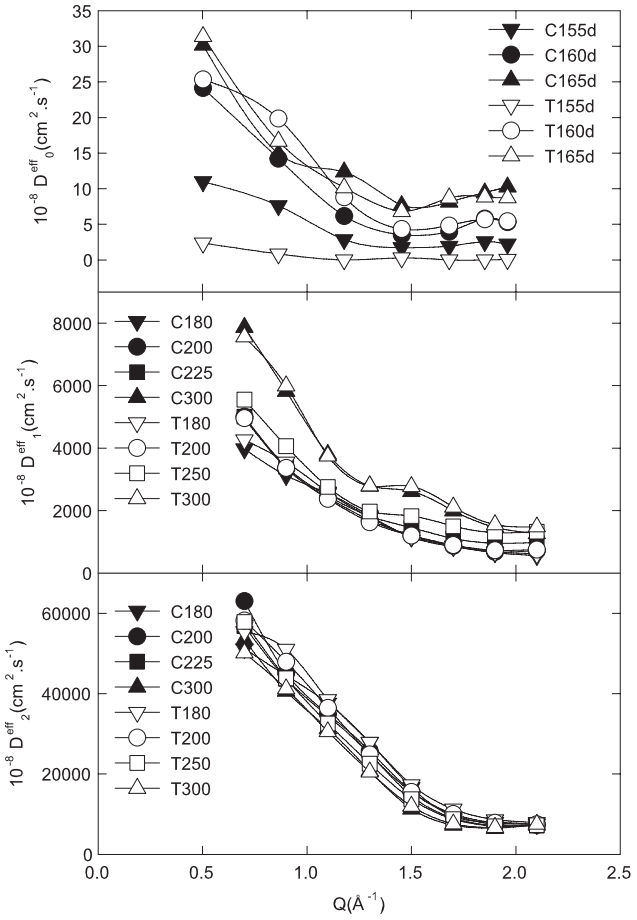

Figure 4. The diffusion function $D^{\text{eff}}(T, Q)$ obtained from the HWHM of the Lorentzian quasielastic peak, Γ, as a function of Q at several temperatures. $D_0^{\text{eff}}(T, Q)$ was measured in the cooling branch of the hysteresis loop in the undercooled liquid region and $D_1^{\text{eff}}(T, Q)$ and $D_2^{\text{eff}}(T, Q)$ in the liquid region (lines are drawn as a guide to the eye, but have no theoretical significance).

a confined volume with a characteristic width $\Gamma_1(Q, T)$ with a slow Q dependence and finally, (c) a last motion, modelled with $\Gamma_2(Q, T)$, that corresponds to some kind of rotation motion in a well defined confined volume with a Q variation around a mean value.

The HWHM of the quasielastic peak $\Gamma(T, Q)$ is a function of T and Q that can alternatively be expressed as a diffusion function $D^{\text{eff}}(T, Q)$ given by

$$\Gamma(T, Q) = \hbar D^{\text{eff}}(T, Q)Q^2. \tag{4}$$

The diffusion function $D^{\text{eff}}(T, Q)$ as a function of Q at several temperatures is shown in figure 4. $D_0^{\text{eff}}(T, Q)$ was measured in the cooling branch of the hysteresis loop in the undercooled liquid region and $D_1^{\text{eff}}(T, Q)$ and $D_2^{\text{eff}}(T, Q)$ in the liquid region. Furthermore $D^{\text{eff}}(T, Q)$ can be factorized as a function of T, $D(T)$ and a function of Q, $K(Q)$

$$D^{\text{eff}}(T, Q) = D(T)K(Q), \tag{5}$$

where $D(T)$ is a temperature dependent diffusion function and $K(Q)$ a Q dependent structure function. $D(T)$ is the mean in Q of $D^{\text{eff}}(T, Q)$ and $K(Q)$ the mean in T of $D^{\text{eff}}(T, Q)/D(T)$.

The thermal variation of the diffusion constant $D(T)$ for the three quasielastic peaks is shown in figure 5. The temperature behaviour of $D_0(T)$, $D_1(T)$ and $D_2(T)$ is different. $D_0(T)$ and $D_1(T)$ increase with the temperature, however, $D_2(T)$ decreases. We fit $D(T)$ with a function of the viscosity of toluene [15]. If $D_1(T)$ and $D_2(T)$ were measured in the liquid phase, $D_0(T)$ was measured in the undercooled phase. However, as we do not know the experimental viscosity in the undercooled phase, we extrapolated the liquid phase values. $D_0(T)$ and $D_1(T)$ depend on T as $T/\eta_0(T)$ while $D_2(T)$ does it as $\eta_0(T)$. In a cage model the diffusion function is given by $D(T) = l^2/\tau$ where l is the jump distance and τ the residence time. Furthermore, for the long-time Brownian motion $\tau = a\tau_{\text{R}}$ where a is a constant bigger than 1 and for the short-time Brownian motion $\tau = b\tau_{\text{B}}$ where b is also a constant bigger than 1. Then, $D(T)$ is fitted by a function of the viscosity or equivalently by a function of the Stokes–Einstein diffusion given by

$$D_0(T) = \frac{l^2 D_{\text{SE}}(T)}{aR^2} \tag{6}$$

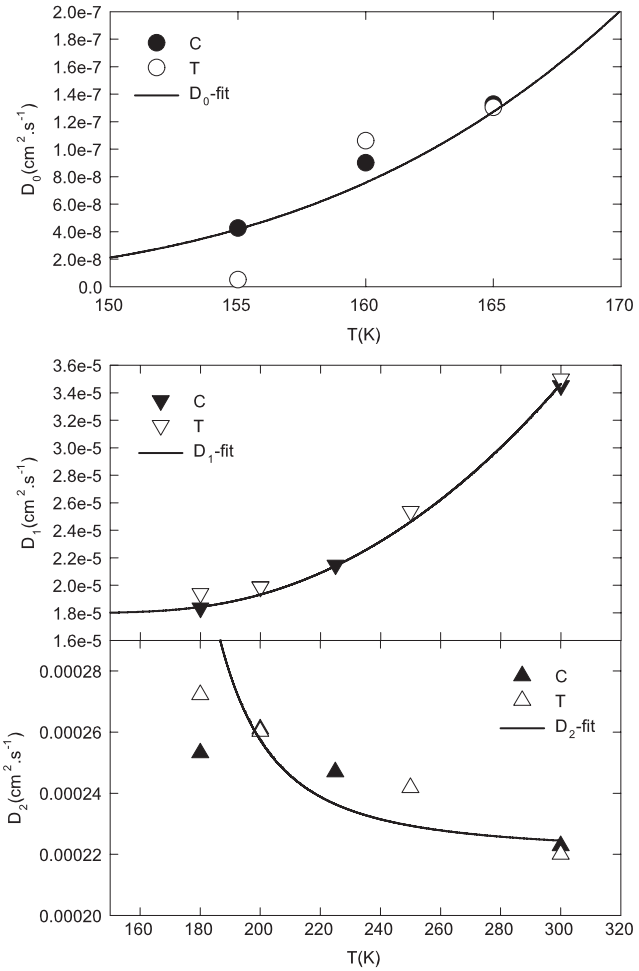

Figure 5. The thermal variation of the diffusion constant $D(T)$ obtained from the factorization of $\Gamma(T, Q)$. The fit of $D(T)$ with a function of the viscosity of toluene is superimposed. See the text for details.

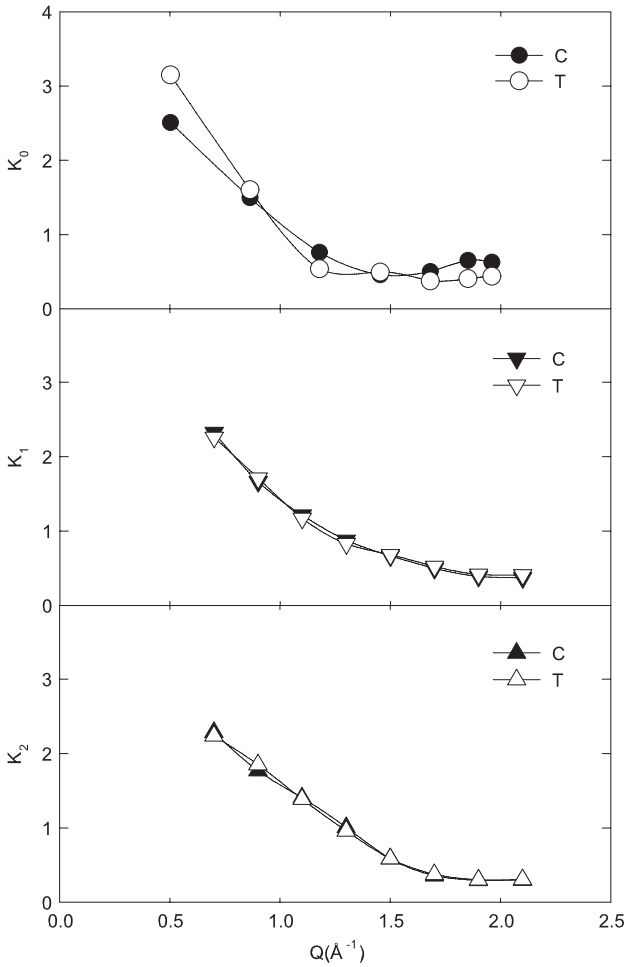

Figure 6. The Q dependence of K_0, K_1 and K_2 for the two samples (lines are drawn as a guide to the eye, but have no theoretical significance).

$$D_1(T) = d_1 + \frac{l^2 D_{\mathrm{SE}}(T)}{aR^2} \tag{7}$$

$$D_2(T) = d_2 + \frac{l^2 k_{\mathrm{B}} T}{bm D_{\mathrm{SE}}(T)}. \tag{8}$$

The fit of these functions is also superimposed on the corresponding $D(T)$ in figure 5. Taking into account the geometrical dimension of our nanotubes: $R = 1$ nm and $L = 650$ nm with a narrow Gaussian distribution, we obtain from the fitting $(l)^2/a = 1.99 \times 10^{-11}$ cm^2, $(l)^2/(bm) = 0.9$ cm^2 g^{-1}, $d_1 = 1.8 \times 10^{-5}$ cm^2 s^{-1} and $d_2 = 2.2 \times 10^{-4}$ cm^2 s^{-1}.

From the temperature behaviour of the diffusion constant we concluded that D_0 and D_1 correspond to a long-time Brownian motion but D_2 to a short-time Brownian motion.

Therefore, it has been shown that the short-time diffusion constant $D_S(T, Q)$ can be written as $D_S(T, Q)/D_{\mathrm{SE}}(T) = H(Q)/S(Q)$ where $H(Q)$ and $S(Q)$ account for the hydrodynamic function and the structure function, respectively. This is not the case for the long-time Brownian motion, but at least for 'hard-spheres' like suspensions it has been shown that $D_{\mathrm{SE}}(T)/D_S(T, Q)$ and $D_{\mathrm{SE}}(T)/D_L(T, Q)$, where $D_L(T, Q)$ is the long-time diffusion constant, although very different in magnitude, have nearly the same Q dependence [16].

The Q dependence of K_0, K_1 and K_2 for the two samples is shown figure 6. The three Ks vary in the same range and are very similar, however there are small differences. K_0 was obtained from measurements in the cooling branch of the high temperature undercooling liquid phase and as the low limit of the hysteresis loop is different for each sample we attributed the difference for K_0 between the two samples to this fact.

In figure 7 the Q dependence of K_1, K_2, K_1/K_2, S and H for the two samples is shown. In the top panel we plot K_1 and K_2 which vary in the same range but present differences as shown in K_1/K_2 in the second panel. In the third panel we present a measure of the structure factor S obtained in an independent measure [17]. Finally in the bottom panel we present H given by $H(Q) = K_1 S(Q)$ for the two samples.

4. Conclusion

We have studied the dynamics of functionalized SWNTs with pentyl ester groups at the ends suspended in deuterated

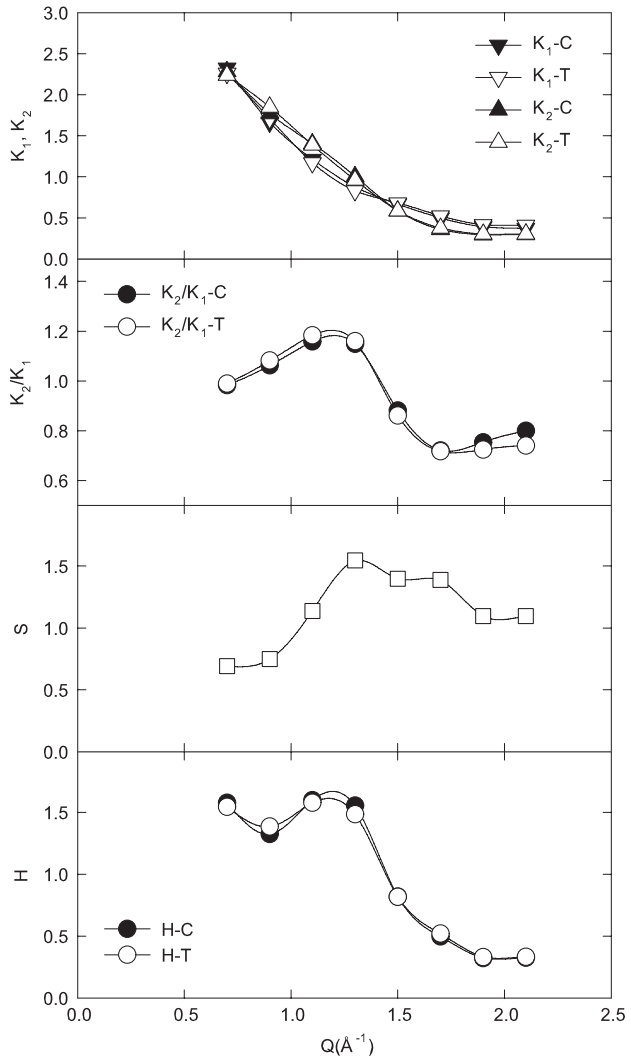

Figure 7. The Q dependence of K_1, K_2 (top panel), K_1/K_2 (middle top panel), S (middle bottom panel) and H (bottom panel) for the two samples (lines are drawn as a guide to the eye, but have no theoretical significance).

toluene with a concentration of 2.6 mg SWNT/1 ml of deuterated toluene. We have performed both IENS and IQNS measurements. Three phases were observed in the temperature range between 4 K and 300 K by IENS measurements: (a) a solid phase for $T < T_g$, (b) an undercooled liquid phase for $T_g < T < T_m$ and (c) a liquid phase for $T > T_m$. Furthermore, in the high temperature range of the undercooled liquid phase hysteresis loops in the heating and cooling scans were observed. The lower limit of the hysteresis loop defines the critical crossover temperature T_c. IQNS measurements in the liquid phase and cooling scan of the undercooled liquid phase were performed. Three different quasielastic peaks were identified. Two in the liquid phase and another one in the undercooled liquid phase. From a comparison of the quasielastic peaks with the viscosity of toluene we conclude that two components are in the long-time range Brownian motion and the other one in the short-time range Brownian motion.

Acknowledgments

We acknowledge very helpful scientific discussions and technical assistance with T Seydel and M Koza (Institute Laue-Langevin), and financial support from Ministerio de Educación y Ciencia (Spain), grants MAT2006-12970-C02-02 and project HOPE CSD2007-00007 (Consolider-Ingenio 2010).

References

[1] Alvaro M, Atienzar P, de la Cruz P, Delgado J L, Garcia H and Langa F 2004 Synthesis and photochemistry of soluble, pentyl ester-modified single wall carbon nanotube *Chem. Phys. Lett.* **386** 342–5
[2] Delgado J L, de la Cruz P, Langa F, Urbina A, Casado J and Lopez-Navarrete J T 2004 Microwave-assisted sidewall functionalization of single-wall carbon nanotubes by Diels–Alder cycloaddition *Chem. Commun.* 1734–5
[3] Rols S, Anglaret E, Sauvajol J L, Coddens G and Dianoux A J 1999 Neutron scattering studies of the structure and dynamics of nanobundles of single-wall carbon nanotubes *Appl. Phys.* A **69** 591–6
[4] Rols S, Benes Z, Anglaret E, Sauvajol J L, Papanek P, Fisher J E, Coddens G, Schober H and Dianoux A J 2000 Phonon density of states of single-wall carbon nanotubes *Phys. Rev. Lett.* **85** 5222–5
[5] Sauvajol J L, Anglaret E, Rols S and Alvarez L 2002 Phonons in single wall carbon nanotube bundles *Carbon* **40** 1697–714
[6] Zhou W, Islam M F, Wang H, Ho D L, Yodh A G, Winey K I and Fisher J E 2004 Small angle neutron scattering from single-wall carbon nanotube suspensions: evidence for isolated rigid rods and rod networks *Chem. Phys. Lett.* **384** 185–9
[7] Bauer B J, Hobbie E K and Becker M L 2006 Small-angle neutron scattering from labeled single-wall carbon nanotubes *Macromolecules* **39** 2637–42
[8] de Heer W A, Bacsa W S, Châtelain A, Gerfin T, Humphrey-Baker R, Forró L and Ugarte D 1995 Aligned carbon nanotube films: production and optical and electronic properties *Science* **268** 845–7
[9] Kymakis E and Amaratunga G A J 2002 Single-wall carbon nanotube/conjugated polymer photovoltaic devices *Appl. Phys. Lett.* **80** 112–4
[10] Echeverría I and Urbina A 2006 Viscoelastic properties of multiwalled carbon nanotube solutions *Eur. Phys. J.* B **50** 491–6
[11] Pusey P N 1991 Colloidal suspensions *Liquids, Freezing and the Glass Transition* ed J P Hansen, D Levesque and Z Justin (Amsterdam: Elsevier) chapter 10
[12] Alba C, Busse L E, List D J and Angell C A 1990 Thermodynamic aspects of the vitrification of toluene, and xylene isomers, and the fragility of liquid hydrocarbons *J. Chem. Phys.* **92** 617–21
[13] Gotze W 1991 Aspects of structural glass transitions *Liquids, Freezing and the Glass Transition* ed J P Hansen, D Levesque and Z Justin (Amsterdam: Elsevier) chapter 5
[14] Wuttke J, Seidl M, Hinze G, Tolle A, Petry W and Coddens G 1998 Mode coupling crossover in viscous toluene revealed by neutron and light scattering *Eur. Phys. J.* B **1** 169–73
[15] Santos J V, Nieto de Castro C A, Dymond J H, Dalaouti N K, Assael M J and Nagashima A 2006 Standard reference data for viscosity of toluene *J. Phys. Chem. Ref. Data* **35** 1
[16] Segre A N and Pusey P N 1997 Dynamic and scaling in hard-sphere colloidal suspensions *Physica* A **235** 9
[17] Jiménez-Ruiz M 2006 private communication